[19] P. Rosa, L. Ricard, P. Le Floch, F. Mathey, G. Sini, O. Eisenstein, *Inorg. Chem.* **1998**, *37*, 3154–3158.

[20] S. Mackay, C. J. Gilmore, C. Edwards, M. Tremayne, N. Stuart, K. Shankland, maXus, University of Glasgow, Scotland, UK, Nonius BV, Delft, The Netherlands and MacScience Co. Ltd., Yokohama, Japan, **1998**.

[21] G. M. Sheldrick, SHELXL-97, Universität Göttingen, Germany, **1997**.

# Investigation of Electronic Communication and Guest Inclusion Using Photoluminescent Macrocyclic Receptors with Ru$^{II}$ Centers and Ph$_2$P–C≡C–C≡C–PPh$_2$ Spacers[**]

Dengfeng Xu and Bo Hong[*]

The study of photoluminescent and redox-active supramolecular systems has attracted recent attention as a consequence of a rapid growing interest in designing artificial arrays for applications in photonic and electronic devices.[1, 2] Systems with various designs have been studied using the assembly of active (for example, metal-based chromophores and redox-active moieties) and passive components (for example, rigid or flexible spacers) as a basis.[1–7] Such systems are constructed to gain a practical insight into parameters and factors that govern processes, such as signal transportation, by electron/energy transfer, electronic and excitonic interaction, as well as guest inclusion and selective molecular sensing.

We have become interested in investigating the photoluminescent and redox-active macrocyclic inorganic cyclophanes for their dual capability in molecular recognition through host–guest interaction and electronic communication between multiple redox centers within a macrocyclic platform. Monomeric model complex [RuCl(tpy)('C$_4$P$_2$')$_2$](PF$_6$) (**1**), rectangular dimer [{RuCl(tpy)('C$_4$P$_2$')}$_2$](PF$_6$)$_2$ (**2**), and triangular macrocycle [{RuCl(tpy)('C$_4$P$_2$')}$_3$](PF$_6$)$_3$ (**3**) have been prepared from [RuCl(tpy)]-based moieties (tpy = 2,2′:6′,2″-terpyridine) and rigid ditopic phosphane spacer Ph$_2$P–C≡C–C≡C–PPh$_2$ ('C$_4$P$_2$'), in order to study the redox interaction and guest inclusion by electrochemical and optical methods. The short alkyne bridge affords the desired structural rigidity to provide controllable cavity sizes in the systems. The Ru$^{II}$-based moieties with polypyridine and polyphosphane ligands also have well-behaved reversible redox properties and photoluminescence characteristics. Such properties are extremely important for the design and applications of new spectral and electrochemical sensory agents for organic guests based on organometallic and coordination receptor systems.[4]

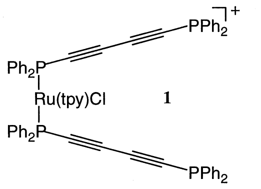

**1**

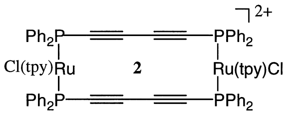

**2**

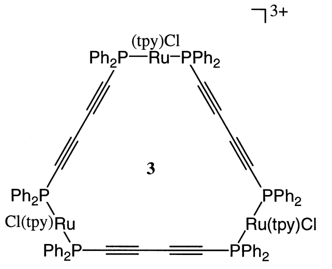

**3**

Herein, the synthesis, chromatographic separation, and characterization of **1**–**3** are reported. Other properties have also been studied, including the ground-state absorption, excited-state emission, redox characteristics, and guest inclusion using anisole and 1,4-dimethoxybenzene as guest molecules. Specifically, the emission intensities of hosts **2** and **3** increase steadily upon addition of guest molecules, and the binding constants of both guest molecules increase significantly when the trimeric system **3** with the larger cavity is used. In addition, the redox interaction between the metal-based corner units is also investigated using cyclic and square-wave voltammetry. The best electronic communication is observed between the two terminal Ru$^{II}$ centers in the doubly bridged complex **2**.

The spacer 'C$_4$P$_2$' is prepared from Me$_3$Si–C≡C–C≡C–SiMe$_3$ by treatment with 2.5 equivalents of MeLi · LiBr and then 2.5 equivalents of ClPPh$_2$. Complexes **1**–**3** are obtained upon reaction of 'C$_4$P$_2$' and [RuCl$_3$(tpy)] (3/1 ratio, with an excess NH$_4$PF$_6$) in refluxing THF/ethylene glycol mixture (4/1), in yields of 15, 30, and 12 %, respectively, after purification. When a 1/1 ratio of 'C$_4$P$_2$' and [RuCl$_3$(tpy)] is used only **2** and **3** (35 and 15 % yield, respectively, after chromatographic separation) are obtained.

The identification of all new complexes was accomplished using $^{31}$P{$^1$H} NMR spectroscopy and electrospray mass spectrometry (ESI-MS). The $^{31}$P{$^1$H} NMR measurements show two peaks at $\delta = +13.6$ (corresponding to the coordinated PPh$_2$ group in 'C$_4$P$_2$') and $\delta = -29.7$ (free PPh$_2$ group in 'C$_4$P$_2$') for **1**. Only one peak at $\delta = +23.1$ for **2** and $\delta = +19.3$ for **3** are observed, both corresponding to the coordinated PPh$_2$ units in the 'C$_4$P$_2$' spacer. ESI-MS measurements offered a straightforward identification of **1**–**3**, giving fragments with single or double positive charges. A representative ESI mass spectrum of **3** is shown in Figure 1, as well as the comparison of the observed and simulated isotope distributions for the doubly charged fragment at $m/z$ 1255.5 [**3** − 2PF$_6$]$^{2+}$.

Cyclic voltammetry (CV) and square-wave voltammetry (SWV) can be used to probe the redox characteristics and electronic communication between the Ru$^{II}$ termini in the macrocyclic molecular systems and the corresponding model complex. Only a single redox peak at +1.06 V (1e$^-$, $\Delta E_p$ = 81 mV) for **1** or +1.30 V (3e$^-$, $\Delta E_p$ = 96 mV) for **3** is observed for the Ru$^{II}$/Ru$^{III}$ redox couples, while two consecutive one-electron redox waves (1:1 ratio, peak separation $\Delta E^0 = E^0_2 - E^0_1 = 100$ mV) are found at +1.03 V (1e$^-$, $\Delta E_p$ = 84 mV) and +1.13 V (1e$^-$, $\Delta E_p$ = 85 mV) for **2** (Figure 2). All redox

---

[*] Prof. B. Hong, D. Xu
University of California, Irvine
Irvine, CA 92697-2025 (USA)
Fax: (+1) 949-824-3168
E-mail: BHONG@UCI.EDU

[**] This work was supported by the US National Science Foundation CAREER Award (CHE-9733546).

0570-0833/00/3910-1826 $ 17.50+.50/0

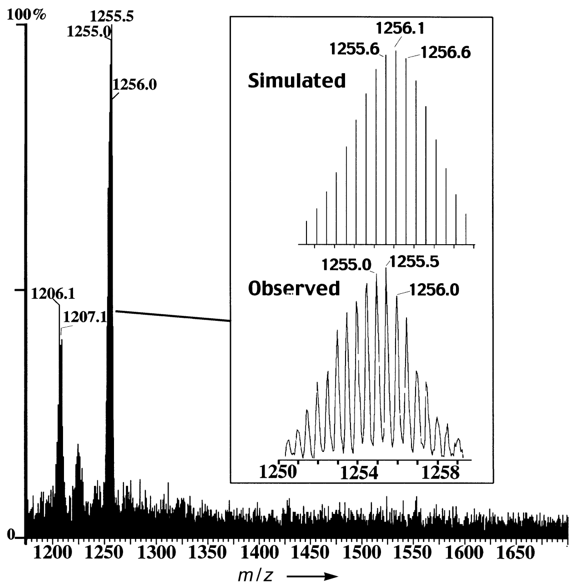

Figure 1. ESI-MS spectrum of **3**. Inset is a comparison of the simulated and observed peaks for $[\mathbf{3} - 2\,\mathrm{PF_6}]^{2+}$. The peak at *m/z* 1206.1 is assigned to $[\mathbf{3} - 2\,\mathrm{RuCl(tpy)} - \text{'}\mathrm{C_4P_2}\text{'} - 3\,\mathrm{PF_6}]^{+}$.

potentials are referenced to the saturated calomel electrode (SCE). Such difference between the redox behavior of **1**–**3** can be ascribed to the different electronic communication in these complexes. All three $\mathrm{Ru^{II}}$ centers in **3**, bridged by single '$\mathrm{C_4P_2}$' spacer, are in electronic isolation and oxidize simultaneously (Scheme 1b), while the two $\mathrm{Ru^{II}}$ centers in **2**, bridged by two '$\mathrm{C_4P_2}$' spacers, communicate much better and give consecutive oxidation peaks (Scheme 1a). As a comparison, a separate study on the redox properties of the linear molecule $[(\mathrm{bpy})_2\mathrm{ClRu}(\text{'}\mathrm{C_4P_2}\text{'})\mathrm{RuCl(bpy)_2}](\mathrm{PF_6})_2$ (**4**) (bpy = 2,2′-bipyridine) also reveals no significant redox interaction between the two $\mathrm{Ru^{II}}$ termini bridged by a single '$\mathrm{C_4P_2}$' spacer and gives two overlapping one-electron redox waves at +1.06 V (versus SCE).[8]

For the complexes that can undergo multistep charge transfer [Eq. (1)] the equilibrium constant ($K_c$) for the comproportionation reaction is defined as shown in Equation (2), with $\Delta E^0 = E_2^0 - E_1^0$ in mV and at 298 K.[9]

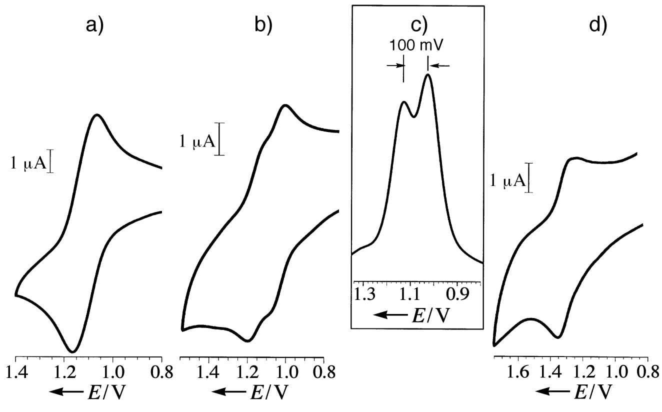

Figure 2. Cyclic voltammograms of **4** (a), **2** (b), and **3** (d) and square-wave voltammogram of **2** (c) obtained at 22 °C in spectrograde acetonitrile, platinum disk (1.0 mm diameter) working electrode, platinum-wire counter electrode, and Ag/AgCl reference electrode. 0.1 M $n\mathrm{Bu_4NPF_6}$ was used as the electrolyte.

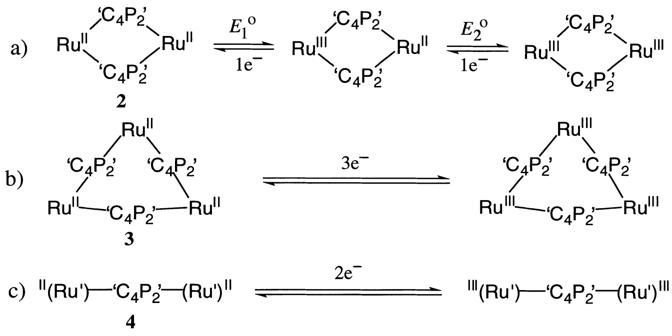

Scheme 1. Description of the redox behavior of **2**–**4**: Ru = [RuCl(tpy)], Ru′ = [RuCl(bpy)$_2$], and '$\mathrm{C_4P_2}$' = $\mathrm{Ph_2P{-}C{\equiv}C{-}C{\equiv}C{-}PPh_2}$.

$$\mathrm{A} \xrightleftharpoons{1e^-,\,E_1^0} \mathrm{B} \xrightleftharpoons{1e^-,\,E_2^0} \mathrm{C} \qquad (1)$$

$$K_c = [\mathrm{B}]^2/[\mathrm{A}][\mathrm{C}] = \exp[(E_2^0 - E_1^0)/25.69] \qquad (2)$$

Here $\Delta E^0 = E_2^0 - E_1^0$ can be estimated from $\Delta E_{1/2}$ measured by CV and SWV studies. A quantitative measure of the energetics for the comproportionation reactions can be achieved from $\Delta E_{1/2}$, and $K_c$ values range from 4 in the uncoupled Robin and Day class I systems to $10^{13}$ in strongly coupled class III systems.[10] The $K_c$ value is calculated as approximately 50 for **2** (Robin and Day class II system), and about 4 for both **3** and **4** (class I). Presumably the two '$\mathrm{C_4P_2}$' spacers between the two $\mathrm{Ru^{II}}$-based termini facilitate the interaction and hence give a better electronic communication in complex **2** than that observed in **3** and **4**, where only one '$\mathrm{C_4P_2}$' spacer is available to mediate the interaction between pairs of $\mathrm{Ru^{II}}$ centers.

The electronic absorption spectra show two intense absorption peaks between 300 and 800 nm, with a chromophore summation effect observed. These two peaks are at 330 nm ($\varepsilon = 12370\ \mathrm{cm^{-1}M^{-1}}$, ligand centered (LC), L is tpy) and 450 nm ($\varepsilon = 3590\ \mathrm{cm^{-1}M^{-1}}$, metal to ligand charge transfer (MLCT)) in **1**. Correspondingly, two peaks at 331 nm ($\varepsilon = 17490\ \mathrm{cm^{-1}M^{-1}}$, LC) and 452 nm ($\varepsilon = 6530\ \mathrm{cm^{-1}M^{-1}}$, MLCT) are observed for **2**, and two peaks at 329 nm ($\varepsilon = 27015\ \mathrm{cm^{-1}M^{-1}}$, LC) and 473 nm ($\varepsilon = 9615\ \mathrm{cm^{-1}M^{-1}}$, MLCT) are obtained for **3**. Comparison of the extinction coefficients of the absorptions in **1**–**3** shows that there is an increase in the extinction coefficients that is proportional to the number of $\mathrm{Ru^{II}}$ centers, although the lower energy peak (MLCT band) in **3** is shifted slightly to a lower energy (Figure 3). Such an increase in the extinction coefficient reflects a chromophore summation effect, and has been previously observed in systems with multiple metal-based chromophores such as metallodendrimers.[11]

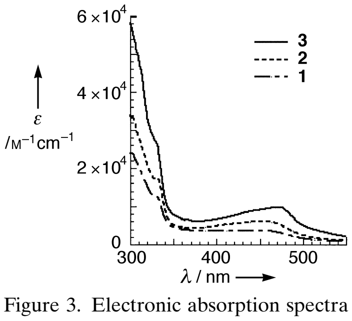

Figure 3. Electronic absorption spectra of **1**–**3** recorded at 22 °C in spectrograde acetonitrile.

A study of the steady-state emission at room temperature shows luminescence at 635, 565, and 550 nm for **1**, **2**, and **3**, respectively, upon excitation at 470 nm. Here, a trend of blue-shifted emissions is observed from monomeric **1** to dimeric **2** and then trimeric **3**. When the guest molecules anisole and 1,4-dimethoxybenzene are added into the solution of the macrocyclic inorganic receptors **2** and **3** in $CH_3CN$, the intensity of the host emission increases steadily (Figure 4). Presumably, the enhanced luminescence effect may derive from altered paths for quenching the excited state of the host molecules upon guest encapsulation. In addition, there is no significant change in the line shape of the host emission during the host–guest study, which implies that the guest affects the luminescence efficiency indirectly.[4a]

We can fit this change of emission intensity as a function of the guest concentration to Equation (3),[4a] to obtain the host–guest binding constant.

$$I = I_0 + \Delta I K_b c/(1+K_b c) \qquad (3)$$

Here $I_0$ and $\Delta I$ are the initial intensity of the emission and the extrapolated maximum change in intensity of the host molecule, respectively, and $c$ is the concentration of guest. The values of the binding constant $K_b$ thus obtained are compared in Table 1. A direct relationship between the cavity size and the host–guest binding constant is observed. The binding constants for both guests anisole and 1,4-dimethoxybenzene in the dimeric macrocycle **2** with the smaller cavity size (cavity dimension $7.2 \times 5.0$ Å$^2$ from molecular modeling study, Table 1) are rather small (between 220–250 $\text{M}^{-1}$). However, the binding constants for both guest molecules increase significantly when the cavity size is increased by using the trimeric **3**. Specifically, the $K_b$ value of anisole (2370 $\text{M}^{-1}$) is larger than that of 1,4-dimethoxybenzene (1390 $\text{M}^{-1}$), which suggests a better fit of the smaller guest molecule anisole in the cavity of **3**. Such a correlation between the cavity size and the host–guest binding constant may suggest the inclusion of guest molecules within the host cavities.[6d]

Table 1. Binding constants of anisole and 1,4-dimethoxybenzene with macrocycles **2** and **3**.

| Complex | $K_b$, anisole [$\text{M}^{-1}$] | $K_b$, 1,4-dimethoxybenzene [$\text{M}^{-1}$] | Cavity dimension[a] [Å] |
|---|---|---|---|
| **2** | 220 | 250 | 7.2 (Ru to Ru)<br>5.0 (P to P) |
| **3** | 2370 | 1390 | 8.9 (Ru to Ru) |

[a] Cavity dimension is determined from molecular modeling calculations. In the rectangular dimer **2** the Ru to Ru and P to P (on the same Ru center) distances are used to define the edges. In the triangular complex **3** the average Ru–Ru distance is used to define the edge of the triangle.

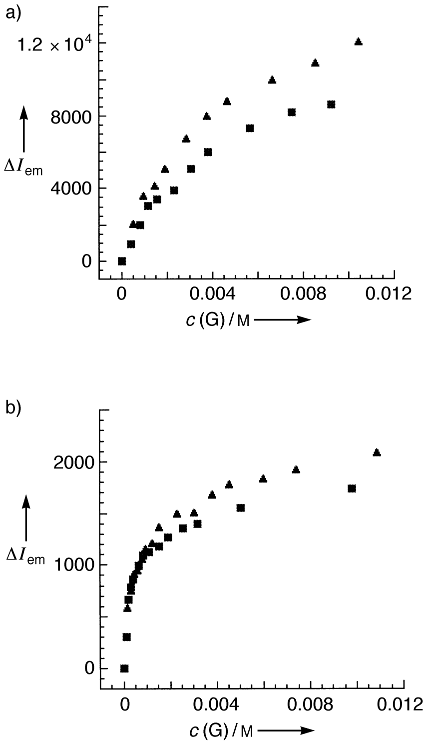

Figure 4. Change of emission intensity of host molecules **2** (a) and **3** (b) as a function of guest concentration recorded at 22 °C in spectrograde acetonitrile, concentration of host molecule: $4.0 \times 10^{-4}$ M for **2** and $1.0 \times 10^{-4}$ M for **3**. Total solution volume change upon addition of guests is < 5 %. ■ = anisole, ▲ = 1,4-dimethoxybenzene.

In conclusion, the new type of photoluminescent and redox-active macrocyclic dimer and trimer with $Ru^{II}$ and ditopic phosphane spacers '$C_4P_2$' were successfully synthesized and characterized. A chromophore summation effect is found in the electronic absorption of the macrocyclic species. A better electronic communication is observed between the two $Ru^{II}$ centers bridged by two '$C_4P_2$' spacers, while the triangular macrocycle **3** displays similar electrochemical behavior to the linear dimeric species **4**. By using the rigid polyphosphane spacer '$C_4P_2$', the cavity sizes in different molecules can also be controlled for selective molecular sensing.

## *Experimental Section*

All reactions are carried out in a $N_2$ atmosphere unless otherwise noted.

'$C_4P_2$': A solution of 1.5 M MeLi · LiBr (2.5 equiv) in diethyl ether was added dropwise to a solution of $Me_3Si{-}C{\equiv}C{-}C{\equiv}C{-}SiMe_3$ (1 equiv) in THF/diethyl ether (1/1) at 0 °C. The reaction was slowly warmed up to room temperature. After 24 h, the resulting slurry of an off-white solid was cooled to 0 °C and treated with $ClPPh_2$ (2.5 equiv). Acetic acid was then added to quench the reaction. The solution was then neutralized with aqueous $NaHCO_3$ solution, and the water layer was extracted with diethyl ether (3 × 75 mL). The combined organic phase was dried over anhydrous $Na_2SO_4$, and the solvent was removed to give a dark brown solid. This solid was washed with acetone (1–2 mL) to give a light-yellow solid. It was then recrystallized from ethanol/chloroform (1/1). Yield: 51 %. $^{31}P\{^1H\}$ NMR (202 MHz, $CDCl_3$): $\delta = -29.2$; CI-MS: $m/z$: 418 [$M^+$], 341 [$M^+ - Ph$], 233 [$M^+ - PPh_2$].

General preparation of **1**–**3**: A suspension of [$RuCl_3$(tpy)] and '$C_4P_2$' (1/3 ratio) in 50 mL THF/ethylene glycol (4/1) was heated to reflux for 2 d. The dark brown solution was cooled down to room temperature. The THF was removed under reduced pressure, and the residue was dropped into a saturated aqueous $KPF_6$ solution (50 mL). The resulting brown precipitate was collected by vacuum filtration, washed with water (3 × 10 mL) and diethyl ether (3 × 10 mL), and dried in vacuo. The solid was purified by column chromatography, using basic alumina and an acetonitrile/toluene eluent. The first portion is **1** (15 % yield) when 1/2 acetonitrile/toluene is used, the second portion is **2** (30 % yield) when 2/3 acetonitrile/toluene is used, and the third portion is **3** (12 % yield) when a 2/1 acetonitrile/toluene eluent is used. $^{31}P\{^1H\}$ NMR ($CD_3CN$, 202 MHz): **1**: $\delta = +13.6, -29.7$; **2**: $\delta = +23.1$; **3**: $\delta = +19.3$; ESI-MS: **1**: $m/z$: 1206.2 [$\mathbf{1} - PF_6$]$^+$, 788.1 [$\mathbf{1}$ – '$C_4P_2$' $- PF_6$]$^+$; **2**: $m/z$: 1720.8 [$\mathbf{2} - PF_6$]$^+$, 787.9 [$\mathbf{2} - 2PF_6$]$^{2+}$; **3**: $m/z$: 1255.5 [$\mathbf{3} - 2PF_6$]$^{2+}$, 1206.1 [$\mathbf{3}$ – 2RuCl(tpy) – '$C_4P_2$' $- 3PF_6$]$^+$, 788.0 [$\mathbf{3}$ – RuCl(tpy)('$C_4P_2$') $- 3PF_6$]$^{2+}$.

Received: December 10, 1999 [Z 14384]

[1] J.-M. Lehn, *Supramolecular Chemistry: Concept and Perspectives*, VCH, Weinheim, **1995**.

[2] a) V. Balzani, F. Scandola, *Supramolecular Photochemistry*, Harwood, Chichester, **1991**; b) V. Balzani, A. Juris, M. Venturi, S. Campagna, S. Serroni, *Chem. Rev.* **1996**, *96*, 759–833.

[3] P. J. Stang, B. Olenyuk, *Acc. Chem. Res.* **1997**, *30*, 502–518.

[4] a) R. V. Slone, K. D. Benkstein, S. Bélanger, J. T. Hupp, I. A. Guzei, A. L. Rheingold, *Coord. Chem. Rev.* **1998**, *171*, 221–243; b) S. M. Woessner, J. B. Helms, J. F. Houlis, B. P. Sullivan, *Inorg. Chem.* **1999**, *38*, 4380–4381; c) M. Fujita, J. Yazaki, K. Ogura, *J. Am. Chem. Soc.* **1990**, *112*, 5645–5647.

[5] a) A. Harriman, R. Ziessel, *Chem. Commun.* **1996**, 1707–1716; b) V. Grosshenny, A. Harriman, M. Hissler, R. Ziessel, *J. Chem. Soc. Faraday Trans.* **1996**, *92*, 2223–2238.

[6] a) B. Hong, J. V. Ortega, *Angew. Chem.* **1998**, *110*, 2210–2214; *Angew. Chem. Int. Ed.* **1998**, *37*, 2131–2134; b) B. Hong, *Comments Inorg. Chem.* **1999**, *20*, 177–207; c) J. V. Ortega, B. Hong, S. Ghosal, J. C. Hemminger, B. Breedlove, C. P. Kubiak, *Inorg. Chem.* **1999**, *38*, 5102–5112; d) D. Xu, H. J. Murfee, W. E. van der Veer, B. Hong, *J. Organomet. Chem.* **2000**, *596*, 53–63.

[7] P. D. Beer, F. Szemes, V. Balzani, C. M. Salá, M. G. B. Drew, S. W. Dent, M. Maestri, *J. Am. Chem. Soc.* **1997**, *119*, 11864–11875.

[8] **4** is prepared by combining '$C_4P_2$' and [$RuCl_2(bpy)_2$] (1/2.2, with excess $NH_4PF_6$) in THF/ethylene glycol (2/1, 30 mL). After refluxing the mixture for 48 h, removing the THF, and adding the residue into saturated aqueous $KPF_6$ solution (50 mL), the yellow solid is collected by filtration (yield 85%, after column chromatography using basic alumina and acetonitrile/toluene as eluent). Analysis of this complex by CV and SWV shows one metal-based redox peak at +1.06 V. D. Xu, B. Hong, unpublished results.

[9] a) D. E. Richardson, H. Taube, *Inorg. Chem.* **1981**, *20*, 1278–1285; b) T. Ito, T. Hamaguchi, H, Nagino, T. Yamaguchi, J. Washington, C. P. Kubiak, *Science* **1997**, *277*, 660–663.

[10] a) C. Creutz, *Prog. Inorg. Chem.* **1983**, *30*, 1–73; b) M. B. Robin, P. Day, *Adv. Inorg. Chem. Radiochem.* **1967**, *10*, 247–270.

[11] a) V. Balzani, S. Campagna, G. Denti, A. Juris, S. Serroni, M. Venturi, *Acc. Chem. Res.* **1998**, *31*, 26–34; b) G. D. Storrier, K. Takada, H. D. Abruña, *Langmuir* **1999**, *15*, 872–884.

## The Absolute Configuration and Asymmetric Total Synthesis of the CP Molecules (CP-263,114 and CP-225,917, Phomoidrides B and A)[**]

K. C. Nicolaou,[*] Jae-Kyu Jung, Won Hyung Yoon, Yun He, Yong-Li Zhong, and Phil S. Baran

The stunning molecular structures[1] coupled with the promising biological activities of the CP compounds (phomoidrides,[2] **1a** and **b**; Figure 1) have inspired numerous studies directed at their total synthesis.[3] In 1999 we reported the first total synthesis of these molecules in their racemic form.[4] Their absolute configuration, however, remained unknown despite the many attempts to prepare and analyze, through X-ray crystallography, a suitably crystalline derivative. After securing the overall structure and configuration at C7[5] of the CP molecules, admirably deduced by Kaneko and co-workers solely from NMR spectroscopic data, we were enticed by the challenge of establishing their absolute configuration. Such knowledge would provide an opportunity to explore modifications of our racemic synthesis and pave the way to optically active CP analogues and mimics, as well as guide future asymmetric total syntheses of these challenging target molecules. Here we report the absolute configuration of the CP molecules as unambiguously determined through chemical synthesis.

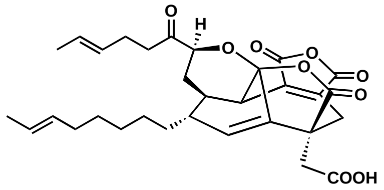

**1a**: (–)-CP-263,114 (phomoidride B)

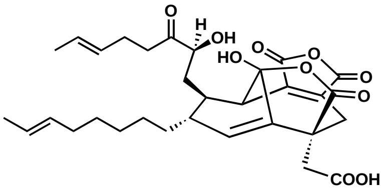

**1b**: (+)-CP-225,917 (phomoidride A)

Figure 1. Absolute configuration of the CP compounds **1** and **2**.

Our reported total synthesis of the CP compounds[4] involved a type-II intramolecular Diels–Alder reaction[6] as a key step to generate the core skeleton of their molecules. Logic dictated that this step (Scheme 1), which converts the

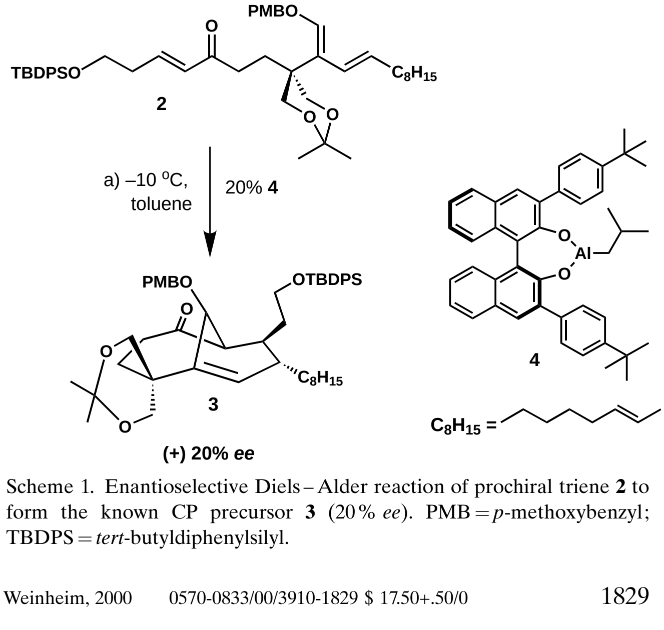

Scheme 1. Enantioselective Diels–Alder reaction of prochiral triene **2** to form the known CP precursor **3** (20% *ee*). PMB = *p*-methoxybenzyl; TBDPS = *tert*-butyldiphenylsilyl.

---

[*] Prof. Dr. K. C. Nicolaou, Dr. J.-K. Jung, W. H. Yoon, Y. He, Dr. Y.-L. Zhong, P. S. Baran
Department of Chemistry and
The Skaggs Institute for Chemical Biology
The Scripps Research Institute
10550 North Torrey Pines Road, La Jolla, CA 92037 (USA)
Fax: (+1) 858-784-2469
and
Department of Chemistry and Biochemistry
University of California San Diego
9500 Gilman Drive, La Jolla, CA 92093 (USA)
E-mail: kcn@scripps.edu

[**] We thank Drs. D. H. Huang, G. Siuzdak, and R. Chadha for assistance with NMR spectroscopy, mass spectrometry, and X-ray crystallography, respectively. This work was financially supported by the National Institutes of Health (USA), The Skaggs Institute for Chemical Biology, doctoral fellowships from the National Science Foundation (P.S.B.) and Boehringer Ingelheim (Y.H.), and grants from Array Biopharma, Boehringer Ingelheim, Schering Plough, Pfizer, Glaxo, Merck, Hoffmann-La Roche, DuPont, and Abbott Laboratories.